Ka-band IQ vector modulator employing GaAs HBTs*

Cao Yuxiong(曹玉雄), Wu Danyu(吴旦昱), Chen Gaopeng(陈高鹏), Jin Zhi(金智)†, and Liu Xinyu(刘新宇)

Institute of Microelectronics, Chinese Academy of Sciences, Beijing 100029, China

Abstract: The importance of high-performance, low-cost and millimeter-wave transmitters for digital communications and radar applications is increasing. The design and performance of a Ka-band balanced in-phase and quadrature-phase (I-Q) type vector modulator, using GaAs heterojunction bipolar transistors (HBTs) as switching elements, are presented. The balanced technique is used to remove the parasitics of the HBTs to result in near perfect constellations. Measurements of the monolithic microwave integrated circuit (MMIC) chip with a size of 1.89 × 2.26 mm^2 demonstrate an amplitude error below 1.5 dB and the phase error within 3° between 26 and 40 GHz except for a singular point at 35.6 GHz. The results show that the technique is suitable for millimeter-wave digital communications.

Key words: Ka band; vector modulator; QPSK; MMIC; HBT

DOI: 10.1088/1674-4926/32/6/065005 **EEACC:** 1250; 1350H

1. Introduction

A conventional modulator is achieved by a complex chain of up-converter mixers, filters and amplifiers; as a result, the cost remains a major factor limiting the widespread use of wireless systems for millimeter-wave applications. Direct carrier modulation at millimeter-wave frequencies has attracted considerable interest as a result of its reduced hardware complexity and cost for wireless applications[1, 2]. A common technique for realizing a direct binary phase-shift keying (BPSK) modulator is to employ a reflection topology using Lange couplers with high electron mobility transistors (HEMTs) or heterojunction bipolar transistors (HBTs) acting as switches on direct and coupled ports[3].

Direct carrier modulation is based on a balanced reflection-type bi-phase amplitude modulator, which is used to remove the amplitude and phase errors of the transistors. Some quadrature phase-shift keying (QPSK) modulators are implemented in the HEMT process[4, 5], however, they require negative bias voltage to perform the modulation function. The advantage of using HBT technology is that it can be integrated with a high efficiency power amplifier (PA) and requires positive bias to operate. Two orthogonal BPSK modulators are connected in phase quadrature to compose a QPSK modulator, which consists of a phase-splitting power-divider that creates either two or four channels, which are individually amplitude modulated and then power-combined in-phase[6].

In this paper, a Ka-band vector modulator monolithic-microwave integrated-circuit (MMIC) is presented. This design employs cold-HBTs to act as variable resistance terminations, Lange couplers to produce an orthogonal signal, and an in-phase 3-dB power combiner (e.g. a Wilkinson combiner) to combine the output signals. Cold-mode HBT device modeling is shown to investigate the practical performance of the modulators. By comparing the characteristics between the simple and balanced modulators from the simulation, it is shown that the balanced technique can remove the parasitics of HBTs effectively. A Ka-band QPSK modulator is realized with two orthogonal balanced modulators in GaAs HBTs and the measurements are carried out.

2. Cold-HBT characterization

A variable resistance element in MMIC technology is the cold GaAs HBT. The HBT process uses a 1-μm GaAs HBT MMIC process on a 4-mil substrate provided by WIN Semiconductors Corporation[7]. The equivalent circuit of a cold-mode HBT device is illustrated in Fig. 1.

A variable voltage to the base terminal controls the collector–emitter resistance R_{ce}. R_{ce} decreases with increasing positive base voltage. Ideally, the cold-HBT has zero collector–emitter resistance at positive bias and infinite resistance below threshold voltage. In practice, however, R_{ce} at positive bias

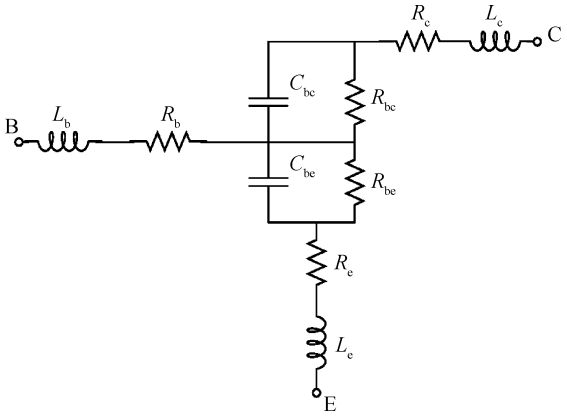

Fig. 1. Equivalent circuit model of the cold-HBT.

* Project supported by the State Key Development Program for Basic Research of China (No. 2010CB327505).

† Corresponding author. Email: jinzhi@ime.ac.cn

Received 9 November 2010, revised manuscript received 4 January 2011

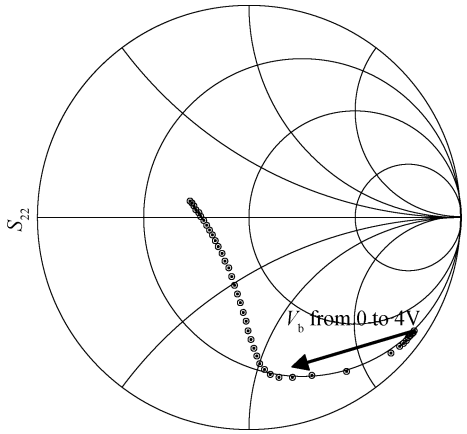

Fig. 2. Output impedance of the cold mode HBT.

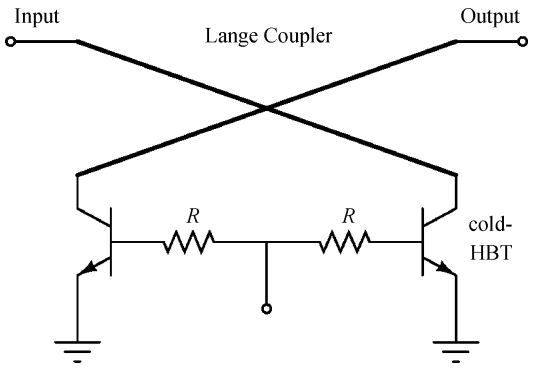

Fig. 3. Circuit topology of a single ended modulator.

is much larger than zero. Although a very large R_{ce} is obtained below threshold voltage, the overall impedance is dominated by the shunt capacitance C_{be} and C_{bc} at high frequencies. The junction capacitances of C_{be} and C_{bc} are not always identical, resulting in highly nonlinear C–V characteristics. Figure 2 illustrates the terminal impedance of the cold mode HBTs versus the base bias voltage sweeping from 0 to 4 V at 36 GHz. The asymmetric output impedance can be observed in Fig. 2.

3. Simple modulator

The simple, single ended modulator used here is based on reflection topology[4], as illustrated in Fig. 3. This topology employs a 3-dB Lange coupler and a pair of cold-HBTs. The input signal, which is split equally into two orthogonal signals by the Lange coupler between the direct and coupled ports, is added to the cold-HBTs. When two orthogonal signals are reflected back to the coupler, they are cancelled at the input port and reinforced at the output port.

For an ideal coupler, the S-parameter matrix of the circuit is given by

$$[S] = \begin{pmatrix} 0 & -\mathrm{j}\Gamma_{\mathrm{T}} \\ -\mathrm{j}\Gamma_{\mathrm{T}} & 0 \end{pmatrix}, \tag{1}$$

where Γ_{T} is the voltage reflection coefficient of the reflection termination.

The output signal of the device is given by

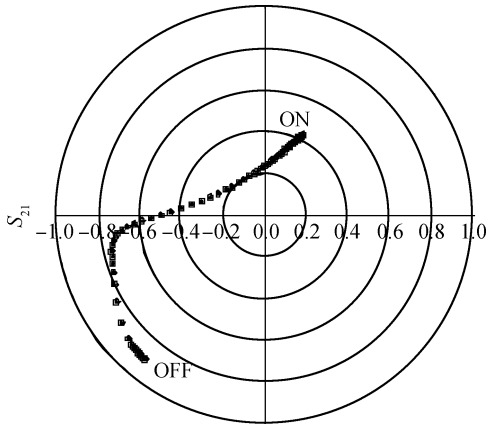

Fig. 4. Simulated S_{21} of a simple modulator.

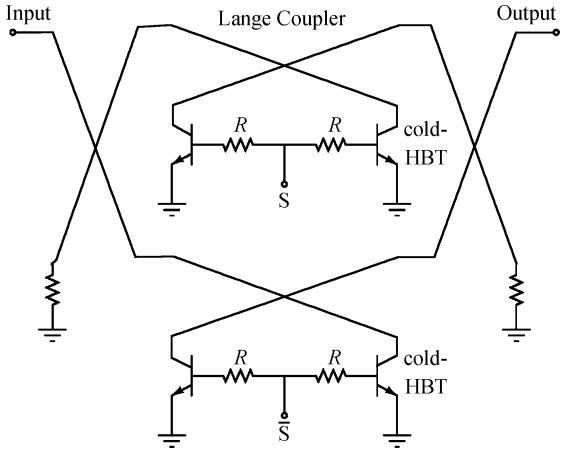

Fig. 5. Circuit topology of the balanced modulator.

$$\angle S_{21} = \angle \Gamma_{\mathrm{T}} - 90°. \tag{2}$$

A Smith's chart plot of S_{21} against bias can be determined by using the above cold-HBT model at 36 GHz, as illustrated in Fig. 4. In this situation, the base voltages were varied from 0 to 4 V and the magnitude plot of S_{21} is shown in Fig. 6(b). It can be seen that the constellation is far from ideal, suffering from both amplitude and phase errors because of the parasitics of the HBTs.

4. Balanced modulator

Single ended modulators are restricted in performance at high frequency due to the parasitics of the HBTs. The amplitude and phase errors caused by the parasitics of the HBTs can be removed by using a balanced technique. The balanced modulator employs two single ended modulators in push-pull mode[8, 9], as illustrated in Fig. 5. The input signal split by the Lange coupler is modulated by the complementary baseband signals (S and $\overline{S}$); the output signal is combined in-phase. The voltage transmission coefficient S_{21} of the balanced modulator is given by

$$S_{21} = \frac{\mathrm{j}}{2}\left(\Gamma_{\mathrm{T}}(S) - \Gamma_{\mathrm{T}}\left(\overline{S}\right)\right), \tag{3}$$

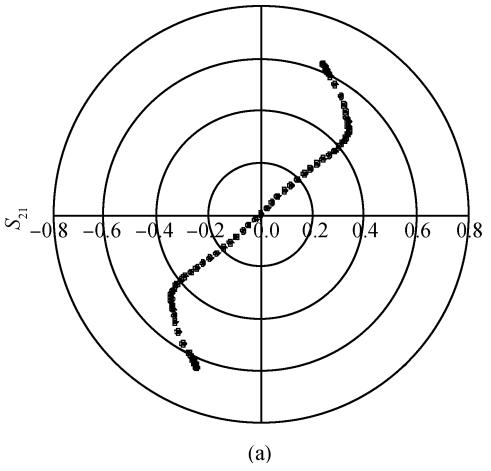

(a)

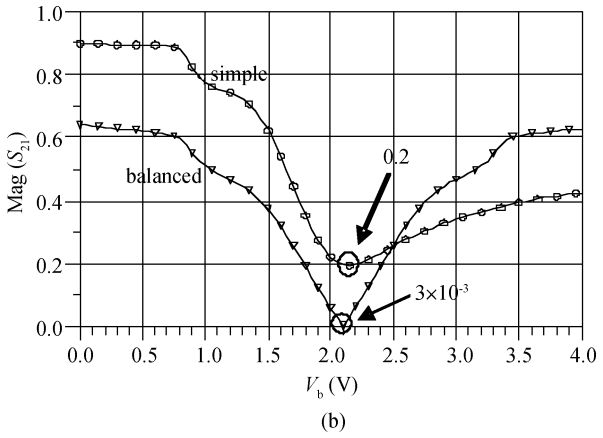

(b)

Fig. 6. Simulated S_{21} of the balanced modulator at 36 GHz. (a) Plot in polar chart. (b) Magnitude attenuation plot.

where S is the bias voltage for the baseband signal, and the relationship of the two complementary voltages is given by

$$\overline{S} = 4.2 - S. \tag{4}$$

The S_{21} of the balanced modulator, as a function of only one varying bias voltage S, is illustrated in Fig. 6(a) at a carrier frequency 36 GHz. In this case, the base bias voltages were varied from 0 to 4 V for each part individually, with the other varied following equation (4). It can be seen that the response is perfectly symmetrical when using push-pull mode. The corresponding attenuation responses of the balanced and simple modulators, as a function of only one varying bias voltage, are illustrated in Fig. 6(b). The minimum voltage wave attenuation of $\sim$0.2 is obtained for the simple modulator, compared with $\sim 3 \times 10^{-3}$ when using a balanced modulator. Therefore, the balanced modulator can remove both amplitude and phase errors caused by the parasitics of the cold-HBTs, even at millimeter-wave frequencies.

5. Ka-band vector modulator design and measured performance

5.1. Vector modulator design

In this way, a vector modulator can be implemented with two balanced modulators[1, 4], as illustrated in Fig. 7. The local oscillator (LO) signal is divided into two equivalent amplitude orthogonal components, which are modulated by the baseband signals. In Fig. 7, I and $\overline{I}$ are the baseband input ports of the in-phase balanced modulator, while Q and $\overline{Q}$ are the baseband input ports of a quadrature-phase balanced modulator. The baseband signals can change the base bias voltages to modulate the LO signal. Summing is achieved using an in-phase Wilkinson power combiner. The I/Q vector modulator can implement multilevel digital modulation schemes, such as QPSK, 16QAM and 256QAM, as well as those used in other applications.

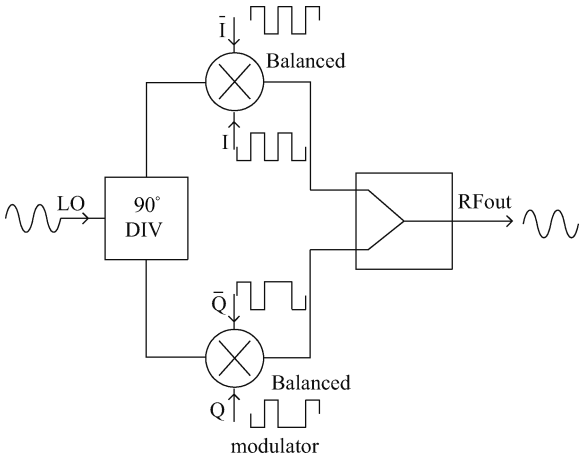

Fig. 7. Schematic of the QPSK modulator.

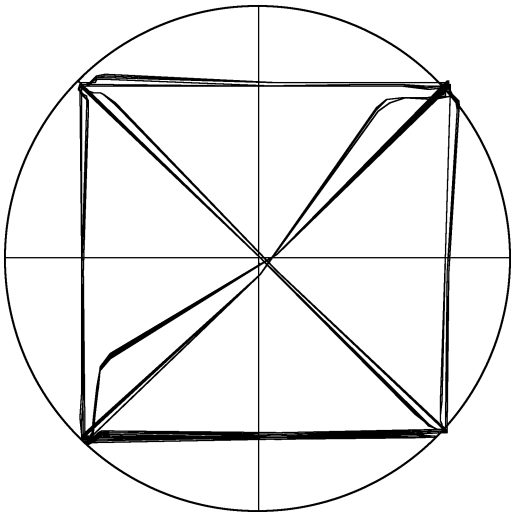

Fig. 8. QPSK constellation at 36 GHz.

Based on the principles presented above, a Ka-band vector modulator was designed using a microstrip on 100-μm-thick GaAs. The passive components, including Lange couplers, a Wilkinson power combiner and interconnection lines, were simulated and optimized by a momentum electromagnetic (EM) simulator in Agilent's Advanced Design System (ADS). The constellation simulation of the vector modulator is shown in Fig. 8. It can be seen that a near-perfect constellation is achieved at 36 GHz, with little amplitude and phase errors.

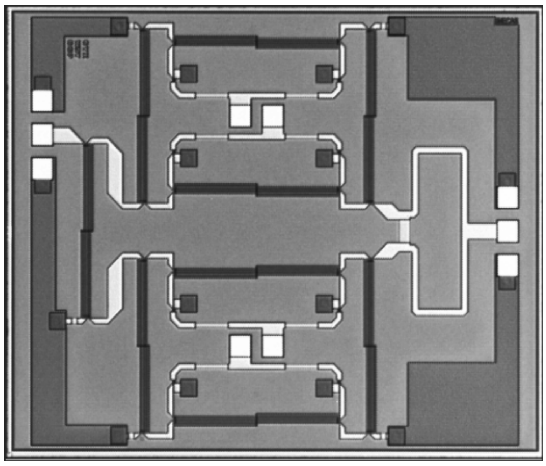

Fig. 9. Microphotograph of the vector modulator.

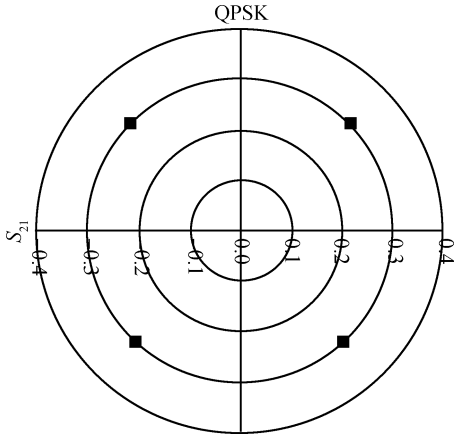

Fig. 10. Corrected measured performance of the QPSK modulator at 36 GHz.

Table 1. Bias voltages for the corrected QPSK modulator at 36 GHz.

I	$\overline{I}$	Q	$\overline{Q}$	Constellation point
2.7	0	3.1	0	0.302/44.892
0	4	0	2.7	0.303/135.546
4	0	0	2.4	0.297/–133.334
1.10	3	3.5	0	0.296/–48.28

5.2. Measurements and discussion

The microphotograph of the vector modulator MMIC designed for operation at 36 GHz, which measures 1.89 × 2.26 mm^2, is shown in Fig. 9. For QPSK modulation, there are four phase states with the same amplitude, which are represented as states of (0, 0), (0, 1), (1, 0), and (1, 1). The measured corrected constellation for QPSK modulation at 36 GHz is illustrated in Fig. 10, and the corresponding voltages used to generate the 4 points are shown in Table 1. The data show excellent results with little amplitude and phase imbalance.

The static S-parameter measurements in the 20–40 GHz frequency range were performed using an Agilent E8363B PNA and a Cascade probe station. The measured S_{21} of four states for the QPSK modulation are plotted in Fig. 11. The amplitude and phase errors of S_{21} are illustrated in Fig. 12. It can be seen that the amplitude error is below 1.5 dB and the phase

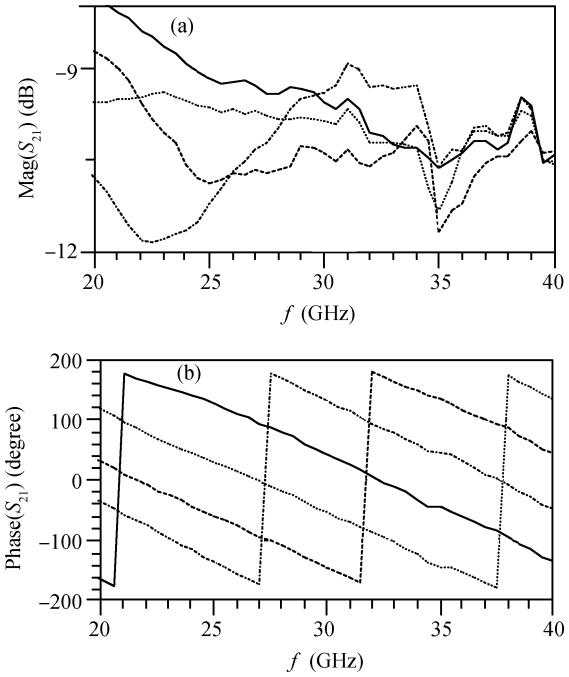

Fig. 11. (a) Insertion loss and (b) phase for the four constellation point versus frequency.

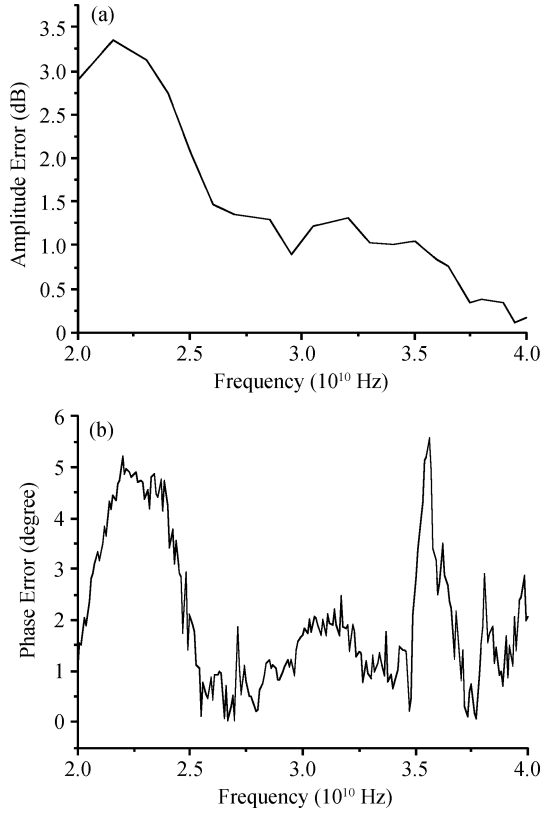

Fig. 12. (a) Amplitude and (b) phase error of the QPSK modulator.

error is within 3° between 26 and 40 GHz, except for a singular point at 35.6 GHz. From the measurements system calibration results, it can be seen that the return losses of the output have a deep notch at 35 GHz. In this case, the measurements system can lead to a small phase and amplitude jitter of S_{21} near

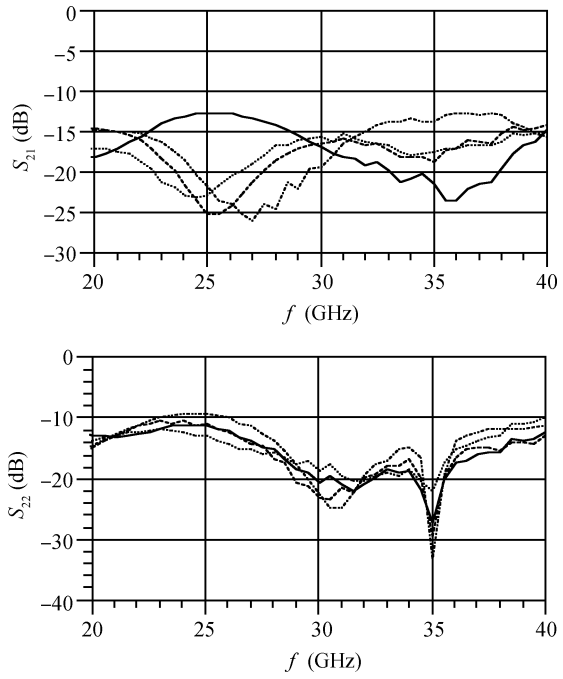

Fig. 13. Return loss for the four states of the QPSK modulator

35 GHz. Therefore, the singular point at 35.6 GHz is due to the measurement equipment.

The input and output return losses are better than 13 dB and 10 dB, respectively, from 26 to 40 GHz, as illustrated in Fig. 13. In these plots, the output return losses have notches at 35 GHz due to the measurement equipment calibration. The bandwidth of the input return loss is wider than the output return loss due to the balanced architecture used in the input port[10].

6. Conclusion

Reflection-type Ka band HBT vector modulator MMIC has been reported in this paper. The MMIC is suitable for broad band digital modulations due to its wide bandwidth, low phase and amplitude errors, and good return losses at the input and output ports. A cold-HBT device model is also developed and verified by comparing simulation results between simple and balanced modulators. The vector modulator using two balanced modulators exhibits excellent constellations for QPSK modulation by carefully tuning the bias voltages at 36 GHz. Therefore, the compact chip provides a low-cost and high performance modulator for microwave applications in the frequency band of 26–40 GHz.

Acknowledgement

The authors would like to acknowledge the assistance of Li Yankui and Ouyang Sihua in adjusting the measurement equipment.

References

[1] Lucyszyn S, Robertson I D. Vector modulators for adaptive and multi-function microwave communication systems. Proc Microwaves Conf, London, UK, 1994: 103

[2] Lucyszyn S, Sewell T, Robertson I D. Multi-level digital modulation performed directly at carrier frequency. Proc 25th European Microwave Conf, 1995, 9: 673

[3] Gokdemir T, Nam S, Ashtiani A E, et al. Millimeter-wave monolithic balanced BPSK modulator using a miniaturized back-wave coupler. IEEE MTT-S, June 1998, 2: 877

[4] Ashtiani A, Nam S I, d'Espona A, et al. Direct multilevel carrier modulation using millimeter-wave balanced vector modulators. IEEE Trans Microw Theory Tech, 1998, 46: 2611

[5] Nam S, Shala N, Ang K S, et al. Monolithic millimeter-wave balanced bi-phase amplitude modulator in GaAs/InGaP HBT technology. IEEE MTT-S Int Microwave Symp Dig, 1999, 1: 243

[6] Kumar S. Directly modulated VSAT transmitters. Microwave Journal, April 1990: 255

[7] GaAs 1 μm HBT model handbook 1.0.1. WIN Semiconduct Corporation, Taoyuan, Taiwan, July 2008

[8] Truitt A, Cerney J, Mason J S. A 0.3–3 GHz monolithic vector modulator for adaptive array systems. IEEE MTT-S Int Microwave Symp Dig, 1989: 421

[9] Pundiah R, Bogaart F V D. MMIC technology sets a new state of the art of microwave vector modulators. Workshop on MMIC's for Space Applications, ESTEC, 1990

[10] Chang H Y, Huang T W, Wang H. Broad-band HBT BPSK and IQ modulator MMICs and millimeter-wave vector signal characterization. IEEE Trans Microw Theory Tech, 2004, 52(3): 908